

Scheimpflug stereocamera for particle image velocimetry in liquid flows

Ajay K. Prasad and Kirk Jensen

A novel stereocamera has been developed based on the angular-displacement method, wherein the two camera axes are oriented in a nonorthogonal manner toward the object plane. The stereocamera satisfies the Scheimpflug condition such that the image plane, the object plane, and the lens plane are nominally colinear. A unique feature of the stereocamera is the introduction of a liquid prism between the object plane and the recording lens, which significantly reduces the radial distortions that arise when imaging through a thick liquid layer. The design of the camera and its computer optimization with geometric modeling are described. Results indicate that the use of a liquid prism reduces the amount of radial distortion by an order of magnitude. The results have been shown to agree very well with experiments.

Key words: Particle image velocimetry, stereocamera, Scheimpflug. © 1995 Optical Society of America

1. Introduction

Conventional particle image velocimetry (PIV) uses a single camera oriented orthogonally to the illuminated plane. The resulting vector field suffers from two deficiencies. First, the out-of-plane velocity component is lost—the vectors are the two-dimensional projections on the object plane of the full three-dimensional vectors. Second, the measured in-plane components are themselves contaminated by perspective error resulting from a local nonzero out-of-plane component; this perspective error ($\Delta x' - \Delta x$) is proportional to the relative magnitude of the out-of-plane component to the in-plane component ($\Delta z/\Delta x$) and the off-axis angle θ , subtended by the scattering particle to the lens (Fig. 1).

Stereoscopic imaging eliminates both of the above shortcomings. Simultaneous views from two different off-axis directions provide sufficient information to extract the out-of-plane component as well as to correct for the errors in the in-plane components.

There are two basic configurations of stereoscopic PIV systems. The translation method uses two cameras whose axes are oriented parallel to each other and orthogonal to the light sheet.¹⁻³ In the translation method, both cameras view a common area encompassing the symmetry line of the two-camera system, but from different off-axis directions. The second configuration, called the angular-displacement method,² uses two cameras whose axes are not parallel, but rotated inward such that they intersect at the midpoint of the domain to be recorded. The translation system and the angular-displacement system are schematically depicted in Fig. 2.

A. Translation Method

When one is measuring a fluid flow whose refractive index is identical to that of air, the implementation of the translation method is straightforward. The object plane, the lens plane, and the image plane are all parallel to each other; thus the magnification is invariant at every location across both image fields. Therefore the vector field resulting from each view can be readily combined (after registration) without the additional manipulations that a variable magnification would necessitate. (A variable magnification would produce two differently stretched image fields, each field requiring interpolation of the data onto a suitably cropped Cartesian grid, before combining the two fields to generate the stereoscopic view.) A further consequence of uniform magnification is that

When this research was performed, the authors were with the Department of Mechanical Engineering, University of Delaware, Newark, Delaware 19716. K. Jensen is now with the Department of Mechanical Engineering, University of Illinois at Chicago, Chicago, Illinois 60607.

Received 31 January 1995; revised manuscript received 27 June 1995.

0003-6935/95/307092-08\$06.00/0.

© 1995 Optical Society of America.

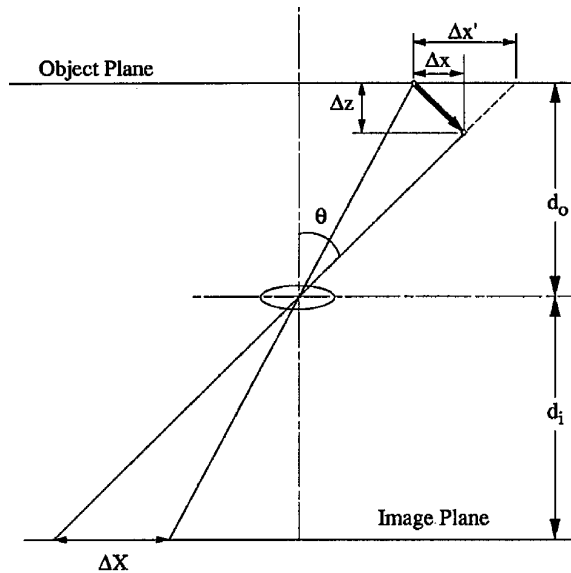


Fig. 1. Error in the measurement of in-plane displacements as a result of out-of-plane motion with a single camera.

the spatial resolution of the resulting three-dimensional vector map is identical to that of the two separate views.

Typically, a translation system gives out-of-plane errors that are 4 times larger than the error in the

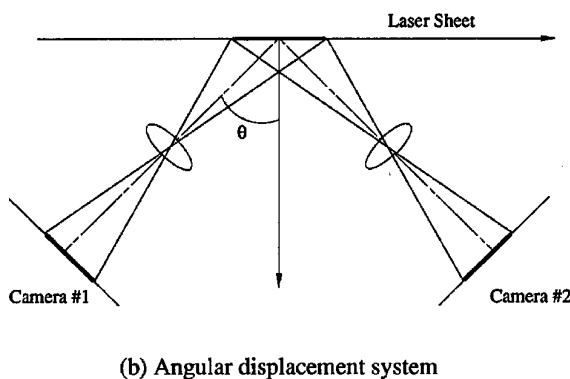
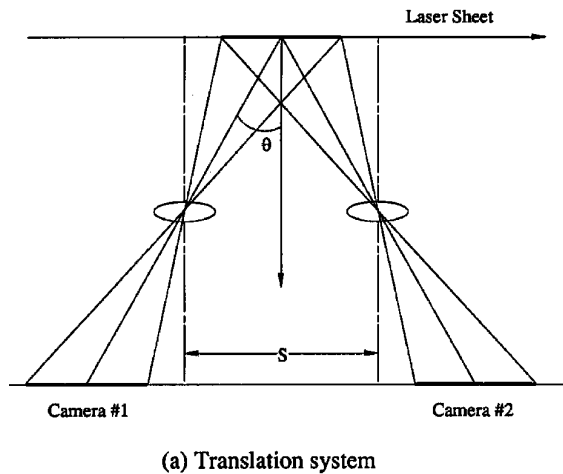


Fig. 2. Two basic configurations for stereoscopic PIV systems: (a) translation method, (b) angular-displacement method.

in-plane measurement. Such a system was used to measure the three-dimensional vectors in an acoustic streaming flow⁴ with air as the working fluid.

When the translation configuration is applied to a liquid flow, the change in the refractive index at the liquid-air interface causes certain difficulties: (i) the region of least confusion is no longer planar; (ii) radial distortions due to the interface produce particle images that are no longer circular, but are smeared in a radial direction (away from the lens axis), resulting in elliptical spots. A detailed description of these difficulties, and the modifications in hardware and software that were used to overcome them, are presented in Ref. 3. Briefly, the hardware modifications included tilting the backplane of the camera to align it better with the surface of least confusion. Consequently, there is a variation (small but not negligible) in the magnification over the image field. The variable magnification then necessitates the mathematical manipulations outlined in the previous paragraph, and these are accomplished through software. Although variable magnification can be accounted for with this procedure, the radial distortions that cause elliptical, blurred images cannot be eliminated. Because it is imperative to reduce the particle-image size for higher accuracy,⁵ it becomes necessary to resort to smaller apertures to reduce the amount of radial distortion. Consequently, a smaller fraction of the scattered energy reaches the recording medium; more powerful lasers are required, leading to the related cost and safety issues.

The modified translation stereoscopic PIV system³ described above was successfully used to measure the three-dimensional swirling flow below a disk rotating in glycerin. Subsequently, this modified system was used to measure the three-dimensional, turbulent flow in thermal convection⁶ with a spatial resolution down to the Kolmogorov scale. However, the nature of the considerations that arise while the translation system is being applied to liquid flows (such as variable magnification) are no different from those that arise with angular-displacement systems, as described below. It is therefore appropriate to ask whether the angular-displacement system may be effectively applied to liquid flows.

B. Angular-Displacement Method

The accuracy of the out-of-plane measurement in a stereoscopic system is proportional to the included angle subtended by the object to the lens center.² In a translation system, this implies a larger separation S between the two lens axes, whereas for an angular-displacement system, this implies a larger angle θ (see Fig. 2). However, there exists an upper bound on the value of S in a translation configuration imposed by the limitations of the lens. Therefore the accuracy of the angular-displacement configuration is, in principle, higher.

Unlike the translation system, the object plane is no longer parallel to the lens plane in the angular-displacement method (see Fig. 2). Therefore it be-

comes more difficult to obtain particle images that are well focused across the image plane. One simple solution is to increase the depth of field of the recording optics. The depth of field δz is given as⁷

$$\delta z = 4(1 + M^{-1})^2 f \#^2 \lambda,$$

where M is the camera magnification, $f \#$ is the f-number, and λ is the wavelength of the illuminating laser. A large depth of field can be obtained at the cost of increasing the f-number, implying that a smaller fraction of the light scattered by the particle will reach the film, or by reducing the magnification. For instance, a small magnification (~ 0.1) was used⁸ to prove the feasibility of a stereoscopic PIV system with CCD cameras as the recording medium.

A second method to obtain images in good focus over the entire image plane is to enforce the Scheimpflug condition,⁹ which requires that the object plane, the lens plane, and the image plane are colinear, as shown in Fig. 3. The use of such a swinging-back camera² removes the depth-of-field restrictions that are prevalent with a fixed-back camera.

Using Fig. 3, we can show that particles in the object plane ($O'C$) will be in sharp focus in the image plane ($O''C$) when their common point of intersection, C , also lies in the lens plane, OC . Placing the origin of the coordinate system at the center of the lens O , we have the following expressions:

for the lens plane,

$$z = 0, \quad (1)$$

for the object plane,

$$z = x \tan \theta - d_o, \quad (2)$$

for the image plane,

$$z = -x \tan \alpha + d_i, \quad (3)$$

where d_o and d_i are the nominal object and image distances, respectively. (In the above expressions, d_o , d_i , θ , and α are all positive quantities.) Any point

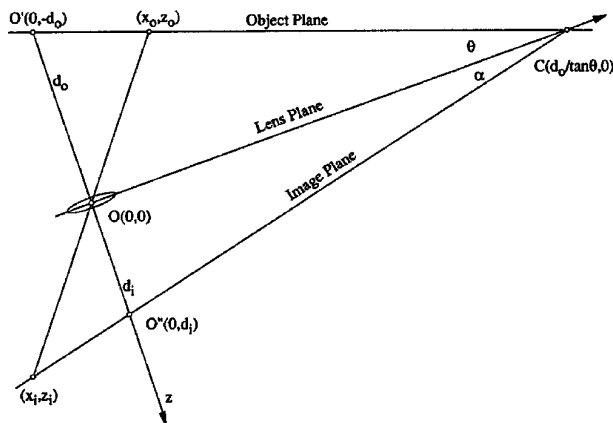


Fig. 3. Schematic depiction of the Scheimpflug condition.

lying in the object plane (x_o, z_o) will form an image at the point (x_i, z_i) as shown in Fig. 3, such that

$$\frac{x_o}{z_o} = \frac{x_i}{z_i}. \quad (4)$$

Using Eqs. (2)–(4), we can readily show that

$$\frac{1}{z_i} - \frac{1}{z_o} = \frac{1}{d_o} + \frac{1}{d_i} \left(= \frac{1}{f} \right), \quad (5)$$

which is the condition that particle images will be in sharp focus in the image plane, f being the focal length of the lens. Of course, the local magnification $-z_i/z_o$ varies across the image plane and only equals the nominal magnification $M = d_i/d_o$ for $x_o = x_i = 0$.

The use of the Scheimpflug condition results in a significantly nonuniform magnification across the image plane (when compared with the much smaller nonuniformity with the modified translation system³). However, these nonuniformities can be accounted for by using the same mathematical manipulations, and indeed the same software, as described in Ref. 3. The second difficulty discussed above, pertaining to radial distortions due to the liquid–air interface, afflicts the Scheimpflug system as well. We are proposing the use of a novel liquid prism to minimize these distortions.

C. Scheimpflug Stereocamera with a Liquid Prism

A common arrangement while measuring liquid flows consists of imaging through a thick liquid layer, such that the object plane is parallel to the liquid–air interface. A conventional PIV system that uses a single camera oriented orthogonally to the interface records particle images that are, for the most part, free of radial distortions owing to the small off-axis angles subtended by the particles to the camera. A stereoscopic arrangement calls for substantially larger off-axis angles and the radial distortions are now readily discernible and can adversely affect accuracy.

One method to ensure that the two cameras continue to enjoy an orthogonal orientation with respect to the liquid–air interface is to redesign the wall of the test section to incorporate a triangular prismatic section. In practice, this may be achieved by constructing a liquid prism, i.e., a thin-walled glass container that is filled with the same liquid, which is then attached to the original, flat wall of the test section. If the glass walls are sufficiently thin, then it is adequate to consider only the one change in refractive index and neglect the others.

The Scheimpflug stereocamera arrangement incorporating a liquid prism is depicted in Fig. 4. The prism is located symmetrically with respect to the stereocamera, and orthogonal viewing is achieved when the half-angle of the stereoscopic system θ equals the angle subtended by the inclined walls of the liquid prism to the original interface. An advantage of using a liquid prism is that it facilitates changes in the stereoscopic viewing angle. It is

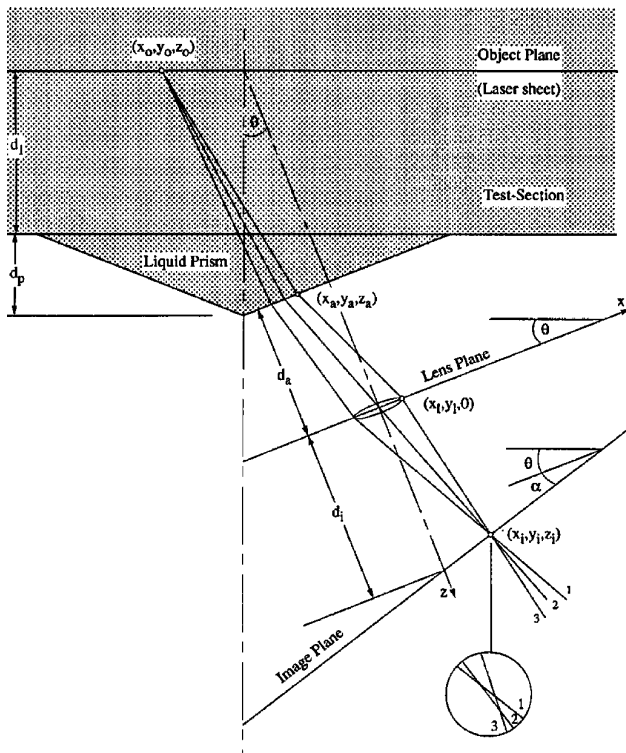


Fig. 4. Scheimpflug stereocamera with a liquid prism (only one of the two cameras is shown).

much easier to fabricate a liquid prism with a different θ than to replace the entire wall of a test section.

In the absence of a liquid-air interface, sharp images are obtained when the object, lens, and image planes are colinear, as indicated by Eqs. (1)–(3). In the presence of a liquid-air interface, colinearity may not yield optimal images because of radial distortion. As in the case of the modified translation camera,³ where the image plane was tilted to align it better with the surface of least confusion, it seems likely that the image plane may require a small deviation from Eq. (3) to ensure optimal focus.

The next section describes a computer model that was developed to optimize the location of the image plane such that particle images were obtained in good focus over the chosen field of view.

2. Modeling

As shown in Fig. 4, the light sheet is oriented such that it is parallel to the viewing wall of the test section and situated at a distance d_l from it. The working fluid has a refractive index μ , and the prism attached to the viewing wall is filled with the same fluid. The angle included by the sides of the liquid prism and the wall of the test section is θ .

The lens axes are oriented orthogonally to the sides of the liquid prism and arranged symmetrically with respect to the liquid prism. (In Fig. 4, only one of the two cameras is shown.) Therefore each lens plane is parallel to the corresponding side of the liquid prism (situated at a distance d_a from it), and the half-angle of the stereoscopic system is also equal to θ .

The size of the liquid prism is determined by the required field of view, as shown in Fig. 4. If the height of the liquid prism is given by d_p , then the nominal object distance is equal to

$$d_o = \frac{1}{\mu} (d_l + d_p) \cos \theta + d_a.$$

For a nominal magnification of M , the image plane is located at a nominal image distance given by $d_i = Md_o$. The Scheimpflug condition fixes the angle α subtended by the image plane to the lens plane as given by $M = \tan \alpha / \tan \theta$. However, as described above, although the Scheimpflug condition predicts sharp imagery at this value of α , radial distortions as a result of the liquid-air interface require small deviations from this condition. The algorithm described next performs an optimization for best focus with two parameters: (i) the nominal image distance d_i and (ii) the image-plane angle α .

In Fig. 4, the light scattered by a particle is refracted at the liquid-air interface, collected by the lens, and then focused at the image plane. Because of the radial distortions, however, light originating from a point source in the object plane will not focus into a point image, but rather into a smeared, or blurred, image. This is depicted in Fig. 4 with three rays, 1, 2, and 3, which cannot intersect at the same point. The amount of distortion depends on μ , d_l , d_p , θ , d_a , M , the location of the particles with respect to the lens axis, and the f-number of the lens (e.g., the smaller the f-number, the larger the lens aperture D and the greater the amount of distortion).

A ray-tracing program was developed to determine the trajectory of light rays originating at a scattering particle of infinitesimal size (to simulate a point source) located at (x_o, y_o, z_o) , refracting at a point on the liquid-air interface (x_a, y_a, z_a) , and entering the lens aperture at a point on its circumference $(x_l, y_l, 0)$. The ray is then focused by the lens and continues onward until it intersects the image plane at (x_i, y_i, z_i) . Thirty-six points were chosen over the circumference of the aperture, and the point of intersection with the image plane of the light ray passing through each circumferential point (and focused by the lens) was determined. The locus of the points of intersection so obtained represents the mapping of the point source into the image plane with only the outermost rays at the lens aperture.

For a given set of input parameters, the process was repeated for different α and d_i . In order to quantify the radial distortion, we computed the area enclosed by the edges of each image. Next we obtained the mean area of all the particle images in the recorded field and normalized it with the nominal area of the recorded field. The configuration was optimal when this mean, normalized area was minimized.

The model developed in this paper assumes an ideal, aberration-free lens. Point sources were used as the scattering particles; finite-size particles were not considered. Likewise, diffraction effects were also neglected; the model is purely geometric. Fur-

thermore, the determination of the area of the particle images did not include considerations such as energy distribution and film response. However, comparison with experiment indicates that although these considerations would somewhat modify the particle-image area, the location of the minimum radial distortion in the (d_i, α) plane is accurately predicted.

3. Results

The baseline case chosen for this study used $\mu = 1.33$, $d_i = 254$ mm, $d_p = 45.7$ mm, $\theta = 16.70^\circ$, $M = 1$, $f\# = 8$, and $f = 120$ mm. The simulations considered a 100 mm wide \times 80 mm high section of the illuminated plane, located symmetrically with respect to the stereoscopic system (and the liquid prism). Ray tracing was performed for point sources located on a square grid with a spacing of 10 mm, giving an 11×9 grid.

The Scheimpflug condition requires (for $M = 1$) that $d_i = 2f = 240$ mm and $\alpha = \theta = 16.7^\circ$. The particle images (magnified 30 times) for this combination of d_i and α are shown in Fig. 5(a). As can be

seen, the particle images exhibit the radial distortion quite clearly; they are stretched in a radial direction, away from the lens axis. However, this combination of d_i and α does not produce a minimum in the total radial distortion over the recorded field. In actuality, this minimum is obtained at $d_i = 242.7$ mm and $\alpha = 13.63^\circ$, and the resulting image field is shown in Fig. 5(b). It is interesting to note that at some locations, the images show a cusplike region, whereas at other locations they show a two-lobe distribution. The lack of perfect focus at the center of the field of view at $(0, 0)$ in Fig. 5(b) is because the nominal image distance d_i is somewhat larger than that of Fig. 5(a). As expected, the original Cartesian 11×9 grid in the liquid is now stretched because of nonuniform magnification over the image field. The grid points in Fig. 5 represent the intersections with the image plane of the chief ray that originates from the point source and passes through the center of the lens.

Figure 6 shows the variation of the image area (normalized by the area of the recorded field) across the image fields shown in Fig. 5 for $y = 0$. For the curve corresponding to Fig. 5(a) it can be seen that the image area goes to zero for $(x = 0, y = 0)$ as expected. However, although the image area is small in the neighborhood of the center of the image field, the image area for large values of $|x|$ (in particular, large negative values of x) is quite high; i.e., the image-area variation shows a large dynamic range. On the other hand, the curve corresponding to the case shown in Fig. 5(b) displays a much smaller dynamic range and a smaller mean image area. Accurate PIV measurements require small and uniform-size particle images, and therefore a small mean and a small dynamic range are both desirable.

Although the particle images in Fig. 5(b) show a more uniform image size (area), the images are certainly not uniform in shape. However, high-

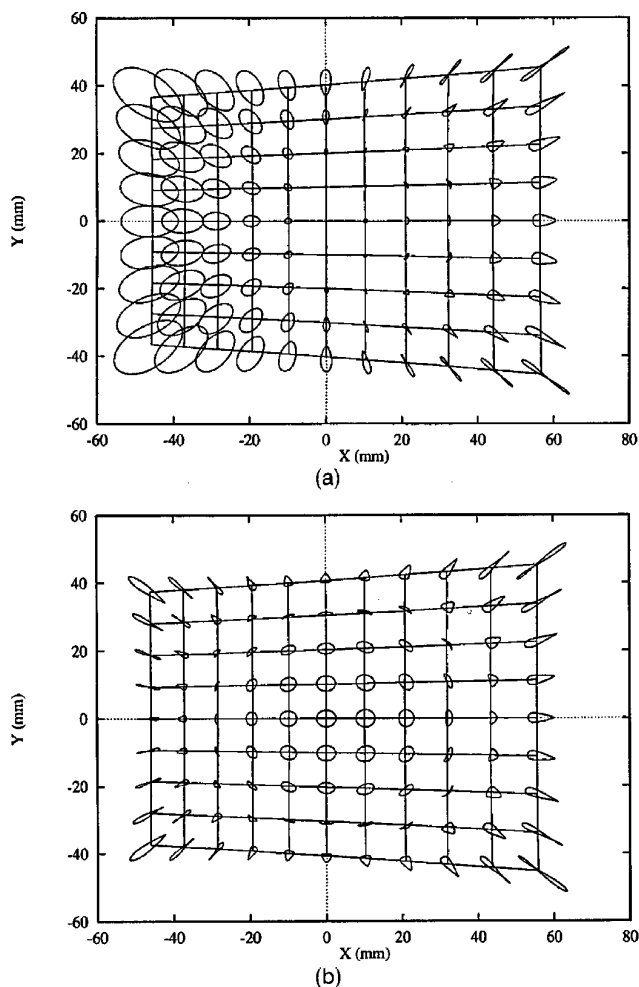


Fig. 5. Radially distorted images (magnified $30\times$) for the Scheimpflug stereocamera with a liquid prism (a) $d_i = 240$ mm, $\alpha = 16.7^\circ$; (b) $d_i = 242.7$ mm, $\alpha = 13.6^\circ$.

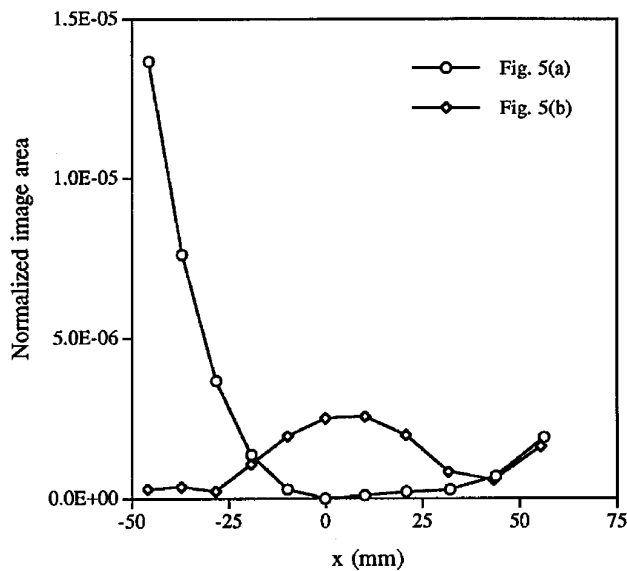


Fig. 6. Variation of image area with x for $y = 0$, corresponding to the image fields in Figs. 5(a) and 5(b).

density correlation PIV is remarkably tolerant of defects in the particle images. Therefore, although the particle images in Fig. 5(b) are quite distorted, especially near the perimeter of the field of view, they may still be usable. If the required accuracy necessitates smaller particle images, then this may be achieved by reducing the f-number, by reducing the magnification, or simply by reducing the field of view. Reducing the field of view even slightly reduces the mean particle-image area substantially because the particle-image distortion grows in a highly nonlinear manner with distance from the lens axis.

The variation of the radial distortion (as given by the mean particle-image area, normalized by the area of recorded field) with α and d_i is shown in Fig. 7. d_i was set to 242.7 mm for the α curve, and α was set to 13.63° for the d_i curve. The value of the minimum error was 2.4×10^{-6} .

The variation of the radial distortion is shown as a function of the f-number in Fig. 8. The f-number has a very strong effect on the magnitude of the radial distortion, especially for $f\# < 8$. The benefit of going to f-numbers greater than approximately 8 is not as significant.

The ray-tracing program developed in this paper to model the Scheimpflug stereocamera can also be used to model the translation system by setting $\theta = 0$. A comparison of the Scheimpflug stereocamera with an equivalent translation system was performed. The parameters for the translation stereocamera were chosen to match those of the baseline Scheimpflug case corresponding to Fig. 5(b) ($\mu = 1.33$, $d_i = 254$ mm, $M = 1$, $f\# = 8$, and $f = 120$ mm). The separation S between the two lens axes was set at 192.95 mm, giving the identical half-angle, $\theta = 16.7^\circ$.

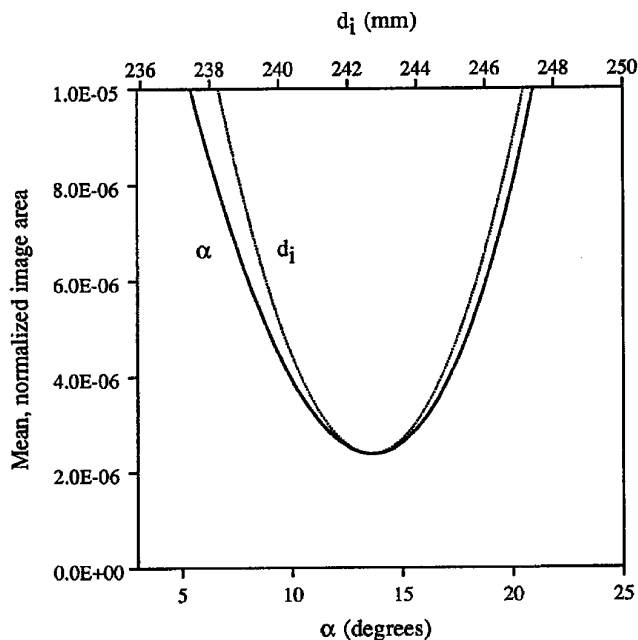


Fig. 7. Variation of radial distortion with image-plane angle α and image-plane distance d_i for the baseline Scheimpflug case.

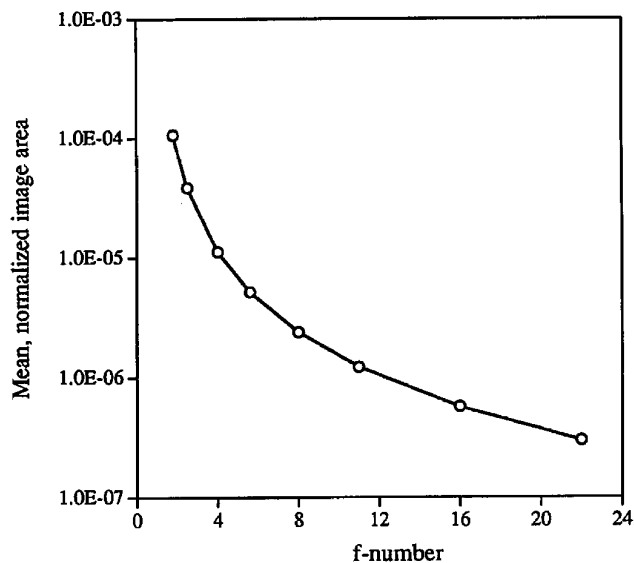


Fig. 8. Variation of radial distortion with f-number.

The simulations also considered a 100 mm wide \times 80 mm high section of the illuminated plane on an 11×9 grid. Figure 9 shows the variation of the radial distortion for this translation stereocamera with d_i and α . The radial distortions were minimized at $d_i = 232.3$ mm and $\alpha = -14.1^\circ$. (Note that the presence of the liquid-air interface causes a sizable deviation from the nominal values of $d_i = 240$ mm and $\alpha = 0^\circ$; second, the optimal value of α is negative, indicating that for the translation system, the direction of tilt is opposite to that of the baseline Scheimpflug case.) The minimum value of the mean, nor-

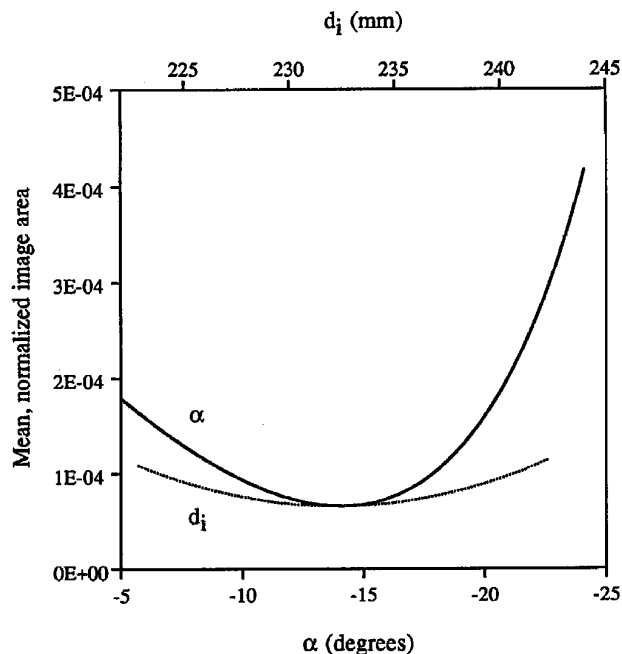


Fig. 9. Variation of radial distortion with image-plane angle α and image-plane distance d_i for the corresponding translation stereocamera.

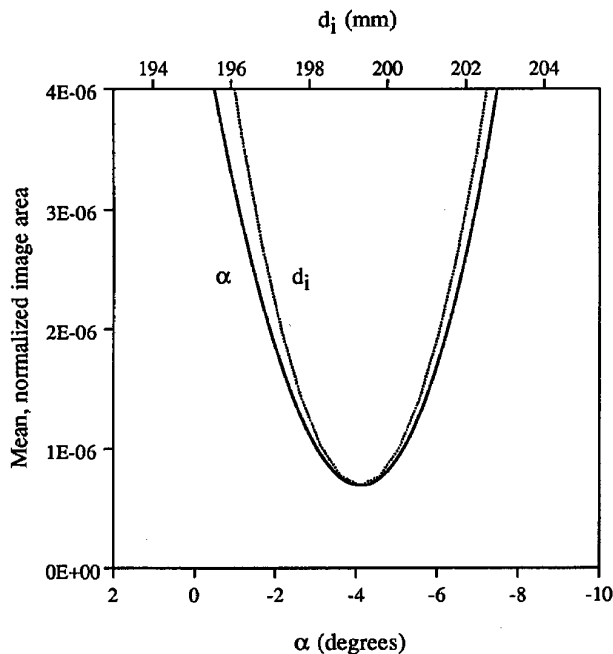


Fig. 10. Variation of radial distortion with image-plane angle α and image-plane distance d_i for the translation stereocamera used in Ref. 6.

malized image area was 6.6×10^{-5} , which is approximately 30 times larger than the minimum error for the corresponding Scheimpflug system (Fig. 7). This implies that the average particle-image diameter is smaller by almost one order of magnitude for the Scheimpflug case. Smaller image diameters are extremely important for increasing the accuracy and the resolution of PIV interrogations, and therefore this result provides confirmation of the benefit of the liquid prism arrangement.

Finally, the program was used to simulate the translation stereocamera used by Prasad and Adrian⁶ in 1993. The corresponding parameters were $\mu = 1.33$, $d_i = 213$ mm, $M = 0.67$, $f\# = 16$, and $f = 120$ mm. The separation S between the lens axes was 140 mm, giving $\theta = 9.9^\circ$. Because the program described in this paper was not available at that time, visual observations were used to determine the optimal values of d_i ($=199$ mm) and α ($= -4^\circ$). Our current simulation has yielded a minimum in the radial distortion at $d_i = 199.3$ mm and $\alpha = -4.1^\circ$ (see Fig. 10). It is reassuring to note the close agreement between the experiment and the simulation. Furthermore, the radially distorted shapes of the particle images produced by simulation showed good qualitative agreement with the actual photographs. A quantitative comparison of particle-image area was made by digitizing the PIV photograph at $9.4 \mu\text{m}/\text{pixel}$ and counting the pixels belonging to specific particles. Measurements were made for $y = 0$ and varying x (Fig. 11). The simulation seems to underestimate the measured values by a constant amount, the difference being approximately 6×10^{-7} . The offset in the two curves is due to the fact that the images on

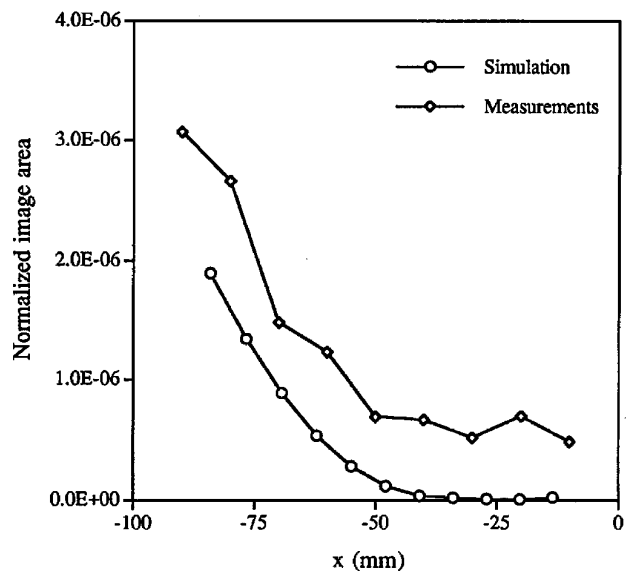


Fig. 11. Measured and simulated particle-image areas for $y = 0$ for the translation stereocamera used in Ref. 6.

the photographs arise from finite-sized particles and include diffraction effects, whereas the simulation considers point sources and neglects diffraction. The difference between the measured and the simulated curves has the expected (positive) sign.

4. Conclusions

A novel liquid prism has been incorporated into a Scheimpflug stereocamera for measuring three-dimensional vectors on a plane with PIV. The introduction of a liquid prism between the test section and the lens permits orthogonal viewing, leading to substantial reductions in radial distortion. The mean particle-image diameter is reduced by approximately one order of magnitude when compared with a similar translation system.

Results show that the radial distortions are a strong function of the f-number for $f\# < 8$. For larger f-numbers, the reduction in radial distortion is not as significant.

The validity of the simulation is confirmed by the close agreement of the present results with experiments. The simplifications used in this study preclude correct absolute values for the particle-image areas; however, the purpose of the simulation is to identify the optimal values of d_i and α . In this respect, the simulation has been successful.

We thank R. J. Adrian for alerting us to the existence of the Scheimpflug condition.

References

1. P. Jacquot and P. K. Rastogi, "Influence of out-of-plane deformation and its elimination in white light speckle photography," *Opt. Lasers Eng.* **2**, 33-55 (1981).
2. V. Gauthier and M. L. Riethmuller, "Application of PIDV to complex flows: measurements of the third component," in *VKI-LS 1988-06 Particle Image Displacement Velocimetry* (Von

- Karman Institute for Fluid Mechanics, Rhode-Saint-Genèse, Belgium, 1988).
3. A. K. Prasad and R. J. Adrian, "Stereoscopic particle image velocimetry applied to liquid flows," *Exp. Fluids* **15**, 49–60 (1993).
 4. M. P. Arroyo and C. A. Greated, "Stereoscopic particle image velocimetry," *Meas. Sci. Technol.* **2**, 1181–1186 (1991).
 5. A. K. Prasad, R. J. Adrian, C. C. Landreth, and P. W. Offutt, "Effect of resolution on the speed and accuracy of particle image velocimetry interrogation," *Exp. Fluids* **13**, 105–116 (1992).
 6. A. K. Prasad and R. J. Adrian, "Investigation of non-penetrative thermal convection using stereoscopic particle image velocimetry," in *Optical Diagnostics in Fluid and Thermal Flow*, S. S. Cha and J. D. Trolinger, eds., *Proc. Soc. Photo-Opt. Instrum. Eng.* **2005**, 667–682 (1993).
 7. R. J. Adrian, "Particle-imaging techniques for experimental fluid mechanics," *Ann. Rev. Fluid Mech.* **23**, 261–304 (1991).
 8. J. Westerweel and F. T. M. Nieuwstadt, "Performance tests on 3-dimensional velocity measurements with a two-camera digital particle-image velocimeter," in *Laser Anemometry Advances and Applications*, A. Dybbs and B. Ghorashi, eds., (American Society of Mechanical Engineers, New York, 1991), Vol. 1, pp. 349–355.
 9. R. E. Altenhofen, "Rectification," in *Manual of Photogrammetry* (American Society of Photogrammetry, Washington, D.C., 1952), p. 457.